Inorganic Chemistry
Article
pubs.acs.org/IC

Group 13 β-Ketoiminate Compounds: Gallium Hydride Derivatives As Molecular Precursors to Thin Films of Ga_2O_3

David Pugh, Peter Marchand, Ivan P. Parkin, and Claire J. Carmalt*

Materials Chemistry Centre, Department of Chemistry, University College London, 20 Gordon Street, London WC1H 0AJ

Supporting Information

ABSTRACT: Bis(β-ketoimine) ligands, $[R\{N(H)C(Me)\text{-}CHC(Me){=}O\}_2]$ (**L_1H_2**, R = $(CH_2)_2$; **L_2H_2**, R = $(CH_2)_3$), linked by ethylene (**L_1**) and propylene (**L_2**) bridges have been used to form aluminum, gallium, and indium chloride complexes $[Al(L_1)Cl]$ (**3**), $[Ga(L_n)Cl]$ (**4**, $n = 1$; **6**, $n = 2$) and $[In(L_n)Cl]$ (**5**, $n = 1$; **7**, $n = 2$). Ligand **L_1** has also been used to form a gallium hydride derivative $[Ga(L_1)H]$ (**8**), but indium analogues could not be made. β-ketoimine ligands, $[Me_2N(CH_2)_3N(H)C(R')\text{-}CHC(R'){=}O]$ (**L_3H**, R′ = Me; **L_4H**, R′ = Ph), with a donor-functionalized Lewis base have also been synthesized and used to form gallium and indium alkyl complexes, $[Ga(L_3)Me_2]$ (**9**) and $[In(L_3)Me_2]$ (**10**), which were isolated as oils. The related gallium hydride complexes, $[Ga(L_n)H_2]$ (**11**, $n = 3$; **12**, $n = 4$), were also prepared, but again no indium hydride species could be made. The complexes were characterized mainly by NMR spectroscopy, mass spectrometry, and single crystal X-ray diffraction. The β-ketoiminate gallium hydride compounds (**8** and **11**) have been used as single-source precursors for the deposition of Ga_2O_3 by aerosol-assisted (AA)CVD with toluene as the solvent. The quality of the films varied according to the precursor used, with the complex $[Ga(L_1)H]$ (**8**) giving by far the best quality films. Although the films were amorphous as deposited, they could be annealed at 1000 °C to form crystalline Ga_2O_3. The films were analyzed by powder XRD, SEM, and EDX.

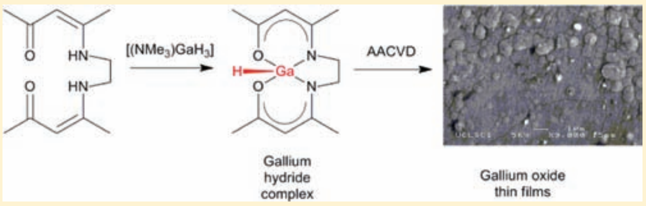

INTRODUCTION

Thin films of gallium oxide, Ga_2O_3, can be used as gas sensors for both reducing gases (e.g., CO, EtOH)[1,2] and oxidizing gases (O_2)[3,4] depending on the sensor temperature. They have been deposited using a variety of methods, e.g., sputtering,[3] spray pyrolysis,[5] and chemical vapor deposition (CVD). Recently, a significant amount of attention has focused on single-source CVD methods where a single molecular precursor, which contains at least one direct Ga−O bond, is used.[6] The most common type of single-source precursor is gallium alkoxides:[7] these compounds have been synthesized in a variety of ways, but the most well-used methods are the reaction of $GaCl_3$ with an alkali metal alkoxide,[8] the reaction of trialkylgallium compounds with an alcohol,[9] the reaction of stabilized gallium hydrides with an alcohol,[10] and the reaction of gallium amide compounds with an alcohol.[11,12] The final method is the most versatile, affording mono-, bis-, or tris-alkoxide compounds of gallium.[13] A comprehensive review of single-source precursors to gallium and indium oxide has recently been published.[14]

Homoleptic β-diketonate complexes of gallium have also been used as precursors, with some, e.g., $[Ga(acac)_3]$ (acac = acetylacetonate), being commercially available.[15−17] However, these precursors are relatively involatile; therefore, high temperatures are needed to volatilize the precursor. To overcome this drawback, we attempted the synthesis of bis(β-diketonate) complexes of gallium and indium with a small third ligand, e.g., hydride. Unfortunately, we found that the high thermodynamic stability of the homoleptic tris(β-diketonate) complexes prevented the isolation of gallium and indium bis(β-diketonate) complexes.[18]

The hydrides of heavy group 13 metals (Ga, In, Tl) are an under-researched area of chemistry, with the main issue being the thermal instability of most of the compounds. However, gallium hydride complexes are low mass and have a clean decomposition pathway; hence a hydride would be an ideal "coligand" for a molecular precursor. The binary hydrides MH_3 (M = Ga, In, Tl) all decompose well below room temperature, with strong Lewis bases needed to stabilize adducts of GaH_3,[19] although a couple of gallium alkoxide hydride complexes have been reported starting from $[GaH_3(NMe_3)]$. The only room-temperature stable adducts of InH_3 have been reported by Jones, comprising bulky trialkylphosphine and NHC (N-heterocyclic carbene) adducts.[20] No TlH_3 complexes are known. A convenient entry point for gallium hydride chemistry is the adduct $[GaH_3(NMe_3)]$, which has limited stability at room temperature.[21]

As described above, precursors to thin films of gallium oxide have evolved from commercially available compounds, such as $[Ga(acac)_3]$, to carefully designed molecules that take into account the requirements of the deposition technique.[14] CVD often requires the precursor to be volatile, although solution-based techniques offer an alternative method of getting the precursor into the gas phase, and here solubility is the key

Received: April 1, 2012
Published: May 17, 2012

Scheme 1. Synthesis of Bis(*β*-ketoimine) Ligands L_1H_2 and L_2H_2 and Bis(*β*-ketoiminate) Metal Complexes 1–8[a]

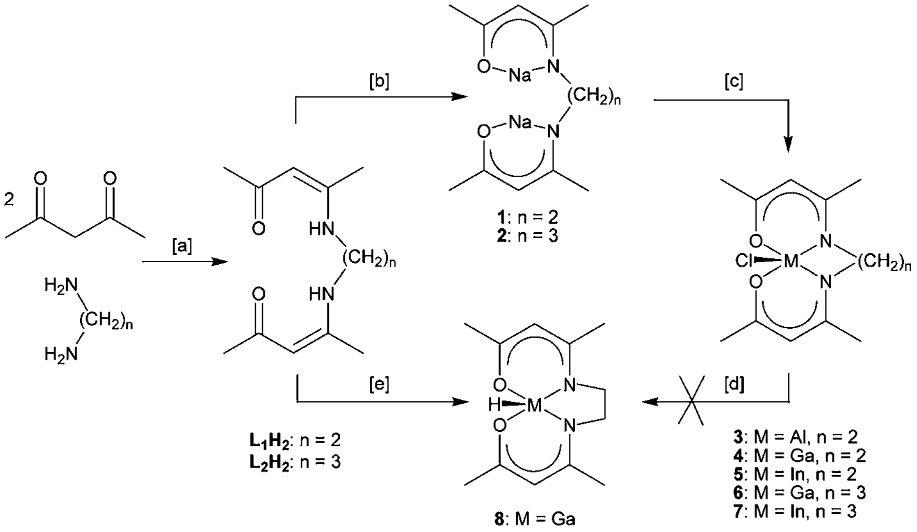

[a] Conditions: [a] solvent free, 150 °C; [b] 2.1 NaH, thf; [c] MCl_3 (M = Al, Ga, In), hexane; [d] LiH/NaH/$NaBH_4$/$LiAlH_4$/$NaBEt_3H$, thf, −78 °C – RT; [e] $[MH_3(NMe_3)]$ (M = Ga, In), Et_2O, −78 °C – RT.

criterion. The *β*-ketoiminate ligand offers a potential means to address the aforementioned issues since the ability to functionalize the imino residue of the ligand means that the thermal stability (and solubility) of the precursor can be increased by tuning the groups attached to the nitrogen atom. Furthermore, it should be possible to isolate monomeric complexes and hence complexes with a high vapor pressure, particularly if hydride is used as the "coligand". Another advantage of employing this ligand type is the potential to enhance the surface reaction between the metal *β*-ketoiminates and the surface of a substrate. However, there have been very few previous reports on the reactivity of *β*-ketoiminate ligands with heavy group 13 metals and none specifically investigating the tuning of the ligand for CVD applications.

Dimethyl-gallium and -indium *N*-aryl-substituted *β*-ketoiminates have been reported, although the presence of an aryl group could lead to carbon contamination of the resulting films.[22] Reaction of a lithiated *β*-ketoiminate with $GaCl_3$ surprisingly resulted only in a *β*-ketoimine adduct of $GaCl_3$, rather than the expected *β*-ketoiminate complex.[23] A donor-functionalized lithium *β*-ketoiminate complex was reacted with $InMe_3$, affording the dimethylindium *β*-ketoiminate species,[24] and the crystal structure of complex **4** (Scheme 1) was previously reported by Vohs et al.,[25] albeit no other characterization data were given. However, none of these compounds have been used as precursors for the CVD of group 13 oxide thin films, nor to stabilize gallium hydrides. Given that current precursors still suffer from chemical instability, poor reproducibility in the growth process, and less than favorable vapor pressures, an investigation into the use of group 13 *β*-ketoiminate complexes as single-source precursors was important given the advantages of the ligand outlined above. In this paper, we report the synthesis of new *β*-ketoimine ligands (and their sodium salts); their reactivity toward group 13 chloride, alkyl, and hydride compounds; and the viability of the new hydride complexes as precursors to thin films of gallium oxide.

■ RESULTS AND DISCUSSION

Compound Synthesis: Bis(*β*-ketoiminates). Ligand $\mathbf{L_1H_2}$ was synthesized according to the literature procedure and was isolated as a beige crystalline solid.[26] Ligand $\mathbf{L_2H_2}$ was synthesized in a similar manner, using 1,3-diaminopropane instead of 1,2-diaminoethane.[27] By reacting a thf solution of $\mathbf{L_1H_2}$ or $\mathbf{L_2H_2}$ with a slight excess of NaH, the disodium salts **1** and **2** were formed (see the Supporting Information). These were isolated as white solids in good yield by removing solvents. However, it was also possible to form complexes **1** and **2** *in situ* before adding the required metal chloride.

A hexane suspension of salt **1** was reacted with $AlCl_3$ in a 1:1 ratio, forming complex $[Al(L_1)Cl]$ (**3**) with concomitant elimination of NaCl. Similarly, complex **4** was synthesized by reacting an *in situ*-generated thf solution of **1** with $GaCl_3$. Compounds **3** and **4** were isolated in reasonable yields as yellow solids with elemental analyses of the solids consistent with the $[M(L_1)Cl]$ formulation. The ^1H NMR spectra of the complexes were similar, showing a backbone CH resonance at *ca.* 5 ppm, ethylene bridge resonances at *ca.* 3.5 ppm, and methyl group peaks around 1.5–2.0 ppm. Complex **3** was crystallized by cooling a toluene solution to −18 °C, but the crystals were of poor quality and were unsuitable for single crystal X-ray diffraction. The solid state structure of complex **4** was previously reported by Vohs et al.[25] The proton resonances of the ethylene bridge in both **3** and **4**, while appearing as a broad singlet in the ^1H NMR spectrum of $\mathbf{L_1H_2}$, were seen as separate resonances in the metal complexes, showing an inequivalence of the two proton environments as a result of coordination to the metal center compared to the equivalent environments for the uncomplexed, freely rotating *β*-ketoimine. The observation of broad singlets in the case of **3** and multiplets in the case of **4** corresponding to the ethylene bridge protons suggests that the molecules possess a degree of fluxionality in solution.

Compound **5**, an indium analogue, was synthesized using the hexane suspension method used for compound **3**. This was crystallized by layering a concentrated CH_2Cl_2 solution with hexane, affording yellow needles, which were suitable for single crystal X-ray diffraction (Figure 1a, Table 1).

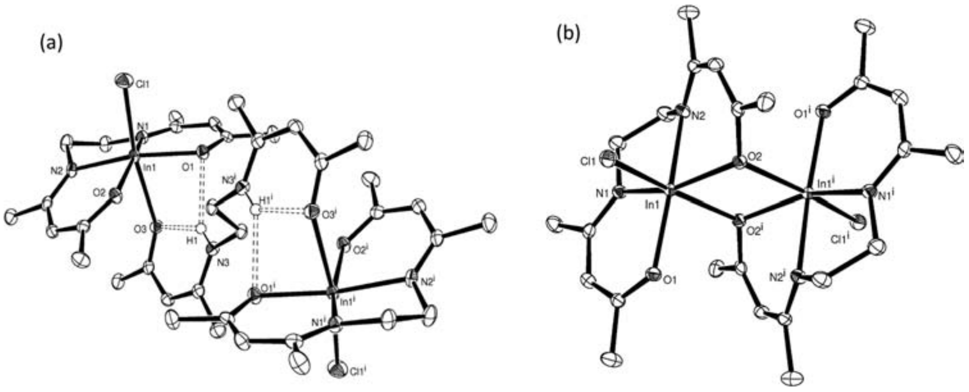

Figure 1. (a) ORTEP diagram showing complex **5a** bridged by one equivalent of ligand $\mathbf{L_1H_2}$. Thermal ellipsoids are drawn at 50% probability, hydrogen atoms (bar H1) omitted for clarity. Hydrogen bonds are denoted by dashed lines, and atoms marked "i" are at the equivalent position ($-x$, $1 - y$, $-z$). (b) ORTEP diagram of compound **5**. Thermal ellipsoids at 50% probability, hydrogen atoms omitted for clarity. Atoms marked "i" are at the equivalent position ($-x$, $-y - 1$, $-z - 1$).

Table 1. Selected Bond Lengths for Compounds 5, 5a, 5·thf, 6, and 7

bond (Å)	**5** (M = In) [In(L_1)Cl]	**5a** (M = In) [In(L_1)Cl]·L_1H_2	**5·thf** (M = In) [In(L_1)Cl]·thf	**6** (M = Ga) [Ga(L_2)Cl]	**7** (M = In) [In(L_2)Cl]
M−O	2.105(2)	2.125(1)	2.097(2)	1.875(1)	2.122(2)[d]
	2.181(2)	2.113(1)	2.101(2)	1.976(1)	2.075(2)[d]
	2.257(2)[a]	2.387(1)[b]	2.413(2)[c]		2.096(2)[e]
					2.113(2)[e]
M−N	2.185(2)	2.186(2)	2.171(2)	1.982(1)	2.164(2)[d]
	2.215(2)	2.182(1)	2.183(2)	2.023(1)	2.181(2)[d]
					2.183(2)[e]
					2.196(2)[e]
M−Cl	2.4420(9)	2.4488(5)	2.4539(8)	2.231(7)	2.3826(7)[d]
					2.4002(7)[e]
C−O	1.303(3)	1.305(2)	1.299(3)	1.2972(19)	1.296(3)[d]
	1.346(3)	1.302(2)	1.293(4)	1.308(2)	1.313(3)[d]
		1.270(2)[b]			1.289(3)[e]
					1.289(3)[e]
C−N	1.321(3)	1.303(2)	1.300(4)	1.309(2)	1.313(4)[d]
	1.297(3)	1.309(2)	1.304(2)	1.323(2)	1.308(4)[d]
		1.328(2)[b]			1.322(4)[e]
					1.310(4)[e]

[a] Bridging In−O bond length. [b] Bond lengths for the neutral ligand. [c] Bond length to thf. [d] Molecule 1 (trigonal bipyramidal geometry). [e] Molecule 2 (square-based pyramidal geometry).

The solid state structure showed that ligand $\mathbf{L_1}$ had bonded to indium in the expected manner through both oxygens and both nitrogens, with a chloride ligand also bound to indium. However, instead of the anticipated five-coordinate In complex, a six-coordinate octahedral species (**5a**) was isolated with one equivalent of ligand $\mathbf{L_1H_2}$ bridging between two In centers through the ketone oxygens. The complex is slightly distorted away from ideal octahedral geometry [*trans* bond angles between 159.68(6)−168.40(3)°] as a result of the relatively large and electronegative chloride group, as well as the short ethylene backbone on $\mathbf{L_1}$. The anionic In−O bond lengths—while slightly different—are significantly shorter than the In−O bond length to the bridging $\mathbf{L_1H_2}$ molecule (Table 1). This is also reflected in the C−O bond lengths, with the delocalized bonding to the indium centers involving O(1) and O(2) resulting in C−O bond lengths that are significantly longer than typical C=O distances. The third oxygen, O(3), being solely a two-electron donor to the indium center, is involved in a much shorter C−O bond length, which is consistent with a typical carbonyl. The proton attached to the amine nitrogen of the neutral ligand is involved in hydrogen bonding both with O(3) on the same ligand and also with the adjacent O(1) of the dianionic ligand. The ^{1}H NMR spectrum is consistent with the presence of two different ligand environments. One set of resonances (including an NH peak at 10.98 ppm) is very close to that of the free ligand; the other set corresponds to the dianionic ligand attached to **5a**. The ratio of the two sets of peaks is 1:2, as expected.

The extra equivalent of $\mathbf{L_1H_2}$ probably came from the incomplete reaction of $\mathbf{L_1H_2}$ with NaH prior to the *in situ* addition of $InCl_3$. In order to prevent the formation of the bridged species, an isolated sample of salt **1** was reacted with $InCl_3$. This afforded a yellow solid in 45% yield, and the ^{1}H NMR spectrum showed only one set of ligand resonances. Crystallization from layering a concentrated CH_2Cl_2 solution of **5** with hexane afforded yellow crystals of compound **5** (Figure 1b, Table 1).

Although the solid state structure confirmed that there was no extra ligand bridging between two metal centers, compound **5** does exist as an oxygen-bridged dimer. The ketoiminate ligand was bound to indium in the expected manner with one chloride *trans* to the bridging oxygen comprising the

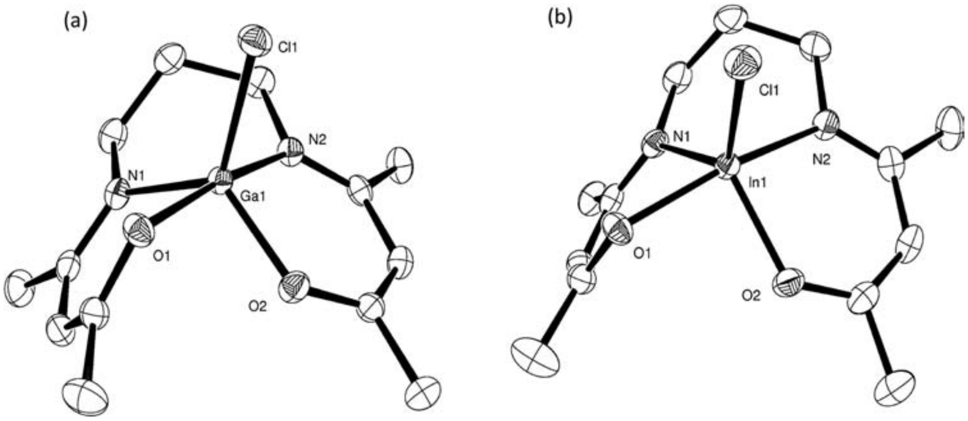

Figure 2. (a) ORTEP diagram of compound **6** and (b) ORTEP diagram showing one of two symmetry-independent molecules (with the severely distorted trigonal bipyramidal geometry) in the asymmetric unit of complex **7**, see Figure S1 (Supporting Information) for the second molecule. Thermal ellipsoids at 50% probability, hydrogen atoms omitted for clarity.

coordination sphere. This was an unexpected result and is probably due to the inflexibility of the 2-carbon bridge in ligand $\mathbf{L_1}$. By restricting the ligand from occupying a sufficient amount of the coordination sphere at indium, it enables a sixth donor group to coordinate to the vacant site, and in the absence of a suitable external Lewis base, dimerization occurs. This is evidenced from the *trans* angles around the indium center which involve $\mathbf{L_1}$: at 155.94(6)° and 164.06(7)°, they are a long way from the ideal 180°.

The In–O bond lengths (Table 1) confirm that the dative bridging In–O bond length is significantly longer than both the anionic In–O bond lengths. Unsurprisingly, there is a marked difference in length of the anionic In–O bonds owing to O(2) being involved in bridging. However, this difference may not be solely a result of O(2) being involved in bridging because the In–N bond lengths are also significantly different from each other. The C–O bonds of $\mathbf{L_1}$ are also different from each other (as are the C–N bonds): this is different from other β-ketoiminate complexes reported in this paper, but not surprising owing to the differences noted for the In–O and In–N bond lengths. The ^{1}H NMR spectrum of **5** was similar to those found for monomeric aluminum and gallium species **3** and **4** such that the inability of the ligand molecule to rotate freely results in an inequivalence of the two proton environments of the ethylene bridge.

The disodium salt **2** was similarly reacted with both $GaCl_3$ and $InCl_3$, forming complexes **6** [Ga($\mathbf{L_2}$)Cl] and **7** [In($\mathbf{L_2}$)Cl] (Scheme 1). Both complexes were isolated as yellow solids and were crystallized by layering concentrated CH_2Cl_2 solutions with hexane. The ^{1}H NMR spectra indicated that $\mathbf{L_2}$ was binding to the metals in the expected manner with no NH proton observed: this was confirmed by structural characterization of both **6** and **7** (Figure 2, Table 1).

Compound **6** crystallized as a five-coordinate slightly distorted trigonal bipyramidal species in the triclinic space group $P\bar{1}$, with $\mathbf{L_2}$ occupying four coordination sites and a chloride completing the coordination sphere. As expected, the largest ligand (chloride) occupies one of the equatorial sites. The degree of distortion away from ideal trigonal bipyramidal can be measured by calculating the τ value, which shows how far a five-coordinate complex is from ideal square-based pyramidal (τ = 0) or trigonal bipyramidal (τ = 1).[28] For compound **6**, the τ value of 0.82 indicates that the degree of distortion away from ideal trigonal bipyramidal is small. This can be seen from the largest bond angle at gallium: the O(1)–Ga(1)–N(2) angle of 172.66(5)° is not far from the ideal 180°.

There is a significant difference in bond lengths between the equatorial and axial groups. The equatorial Ga–O length [1.875(1) Å] is much shorter than the axial Ga–O bond length [1.976(1) Å], and a similar effect is observed with the Ga–N bond lengths, albeit the difference of 0.04 Å is not as marked as the case for the Ga–O bonds (0.1 Å). However, this difference is not manifested in the C–O bond lengths, which are identical within experimental error. They are also identical to the delocalized C–O bond lengths in compound **5a**, despite the smaller ionic radius of Ga^{3+} compared to In^{3+}. However, there is a very small difference between the C–N bonds, and the longer of the two bonds is also slightly longer than the delocalized C–N bonds in complex **5a**.

Compound **7** also crystallized as a five-coordinate species in the triclinic space group $P\bar{1}$ with $\mathbf{L_2}$ again occupying four of the coordination sites with a chloride ligand occupying the fifth. Although the molecular structure is extremely similar to that of compound **6**, with the only difference being the slightly larger In(III) cation in place of Ga(III), there is a significant difference in the manner in which compound **7** crystallizes, with two symmetry-independent molecules in the asymmetric unit. This results in an overall Z value of 4 as opposed to 2 in compound **6**. The two independent molecules occupy vastly different geometries, with the molecule centered around In(1) existing in a severely distorted trigonal bipyramidal geometry (τ = 0.70; Figure 2), whereas the molecule centered around In(2) adopts an almost ideal square-based pyramidal geometry (τ = 0.03; Figure S1, Supporting Information). The origin for this is not clear, but the fact that compound **6** does not exhibit a similar distortion may indicate a more significant reason than simply crystal packing effects.

The In–O bond lengths across both molecules are in a range between 2.075(2) and 2.122(2) Å, but each molecule contains one "longer" In–O bond and one "shorter" In–O bond, with the difference between the two being statistically significant for each molecule. The same is true of the In–N bond lengths with the "longer" and "shorter" In–N bonds for each molecule being significantly different. However, the C–O bonds for each molecule are not different within experimental error, and the same is true for the In–N bonds (Table 1).

The ^{1}H and ^{13}C NMR spectra for **6** and **7** both supported the formation of the desired monomeric complexes. Similarly to that seen for **3**, **4**, and **5**, a separation of the two NCH_2 resonances of the propylene bridge was observed in both cases as a result of coordination to the gallium (**6**) and indium (**7**) centers, showing an inequivalence of the proton environments. The broad resonances seen again suggest fluxional behavior of the molecules in solution.

Compounds **4** and **5** were both reacted with a variety of hydride sources (LiH, NaH, $NaBH_4$, $LiAlH_4$, $NaBEt_3H$) in an attempt to replace the chloride ligand with hydride. However, in all cases, no reaction was observed, and the ^1H NMR spectrum merely indicated that starting material remained. In order to try to remove the chloride ligand completely, a THF solution of compound **5** was reacted with one equivalent of freshly formed C_8K. Although no color change was observed, slow diffusion of hexane into the THF solution of the reaction product yielded yellow crystals, which were suitable for single crystal X-ray analysis (Figure 3, Table 1).

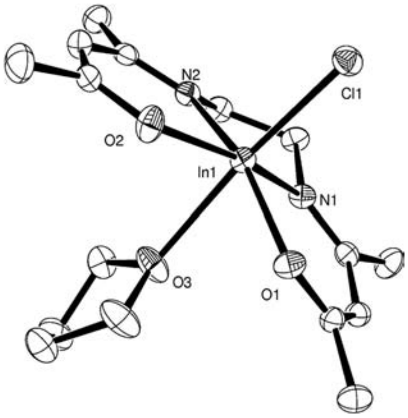

Figure 3. ORTEP diagram of compound **5·thf**. Thermal ellipsoids at 50% probability, hydrogen atoms omitted for clarity.

Compound **5·thf** crystallized as an octahedral species with one equivalent of L_1, one chloride ligand, and one thf molecule comprising the coordination sphere. The chloride and thf ligands are mutually *trans* with the four ligand donor atoms to the metal existing in a single plane [RMS deviation for O(1), O(2), N(1), N(2) = 0.0455 Å]. The metal atom is out of this plane by 0.277(1) Å. The In−O bond lengths involving the ligand are identical within experimental error, as are the In−N bonds, although there is a marked difference between the In−O bonds from the ligand and the In−O bond of the thf ligand. They are also very similar to the In−O and In−N bonds found in complexes **5a** and **7**. This is also borne out by the C−O and C−N bonds, which are identical within experimental error.

Although it is surprising that compound **5** did not react with C_8K, it is probable that carrying out the reaction in thf caused complex **5·thf**, which is kinetically inert, to form prior to the reaction with C_8K. However, switching the solvent to Et_2O and repeating the reaction of **5** with C_8K also did not lead to any reaction taking place.

Owing to the unreactivity of compound **4**, in order to prepare a gallium hydride derivative of ligand $\mathbf{L_1H_2}$, it was reacted directly with a freshly prepared ethereal solution of $[GaH_3(NMe_3)]$ (Scheme 1). A pale yellow solution with a white suspension formed, and the solid was removed by filtration. Compound **8** was isolated as a yellow powder in 71% yield by removal of the volatiles, and the ^1H NMR spectrum showed no resonance associated with the NH proton, in addition to a small peak at 5.56 ppm characteristic of gallium hydrides. All attempts at crystallizing compound **8** only resulted in the formation of a microcrystalline solid unsuitable for single crystal X-ray diffraction, but elemental analysis was consistent with the formation of compound **8**.

In an attempt to synthesize an indium analogue of compound **8**, ligand $\mathbf{L_1H_2}$ was reacted with a freshly prepared ethereal solution of $[InH_3(NMe_3)]$ (Scheme 1). At −78 °C, no reaction was observed, but upon slow warming to RT, a gray precipitate of indium metal formed in a pale brown solution. After filtration and removal of the solvents, ^1H NMR spectroscopic analysis found that the brown solution only contained ligand $\mathbf{L_1H_2}$. While complexes of the type $[InH(L)_2]$ (L = formamidinate) have been previously isolated,[29] in our case, it is unknown whether any reaction between $\mathbf{L_1H_2}$ and $[InH_3(NMe_3)]$ took place: given the kinetic and thermal sensitivity of indium hydride complexes, it is possible that the indium hydride starting material decomposed before any reaction took place. The use of isolated $[InH_3(NHC)]$[30] as a starting material did not lead to the formation of $[InH(L_1)]$, with no reaction observed to take place.

Compound Synthesis: Donor-Functionalized *β*-Ketoiminates. Compounds such as $[Ga(O^iPr)_3]$ usually exist as oligomers, but by using donor-functionalized alkoxides (which have a Lewis base attached to the alkoxide moiety), it is possible to isolate monomeric and dimeric alkoxides.[31,32] Through a judicious choice of the primary amine, it should

Scheme 2. Synthesis of Donor-Functionalized *β*-Ketoimine Ligands L_3H and L_4H and Donor-Functionalized *β*-Ketoiminate Complexes 9−12[a]

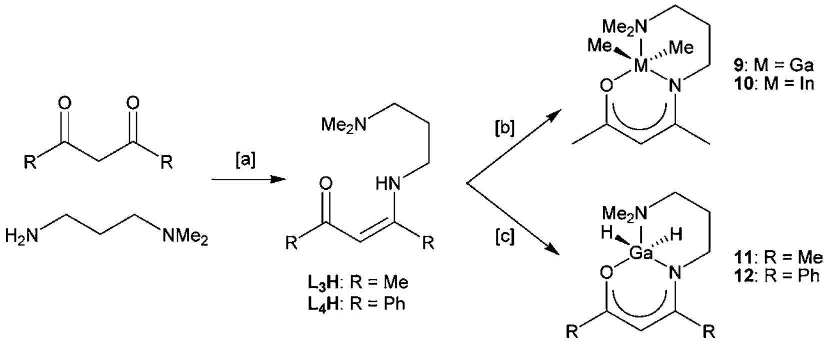

[a]Conditions: [a] solvent free, 150°; [b] MMe_3 (M = Ga, In), toluene, 110 °C, 16 h; [c] $[GaH_3(NMe_3)]$, Et_2O, −78 °C − RT.

be possible to form a β-ketoimine ligand with an extra Lewis base, i.e., donor-functionalized β-ketoiminates. The presence of the extra Lewis base should lead to coordinative saturation of the metal center, enabling isolation of additional hydride species. Hence, $\mathbf{L_3H}$ (R = Me) was synthesized by combining acetylacetone with N,N-dimethylpropylenediamine, then heating the mixture to 150 °C for four hours (Scheme 2). After cooling and extraction into diethyl ether, drying over anhydrous Na_2SO_4 removed sufficient residual water such that no H_2O signal was observed in the ^1H NMR spectrum of the crude product. Indeed, the crude product (an orange oil) was of sufficient purity for further reactivity studies. Ligand $\mathbf{L_4H}$ (R = Ph) was synthesized in a similar manner, starting from dibenzoylmethane instead of acetylacetone. The product was isolated as an extremely viscous orange-brown oil, again with no purification step necessary as judged from the ^1H NMR spectrum. In both cases, the NH peak was observed at a very downfield position of 10.75 ppm ($\mathbf{L_3H}$) and 11.87 ppm ($\mathbf{L_4H}$). Coupling of the NH proton to the CH_2 group was also observed, with the signal corresponding to the latter group appearing as a doublet of triplets at 3.20 ($\mathbf{L_3H}$) and 2.99 ($\mathbf{L_4H}$) ppm.

In an attempt to gauge the reactivity of ligand $\mathbf{L_3H}$, it was reacted with one equivalent of $GaMe_3$ in Et_2O at −78 °C. After warming to RT and stirring for 16 h, removal of all volatiles afforded a gelatinous pale brown oil. ^1H NMR spectroscopy of the oil revealed a reaction had taken place, but two products (in a 1:1 ratio) were present. By analyzing the integrals of the peaks in the Ga−Me region of the spectrum (*ca.* 0.0 ppm) relative to that for the CH peak on the backbone (*ca.* 5.0 ppm), in addition to the peak corresponding to the CH_2 group next to the amine NH (or N^-), it was determined that the two products were (i) a simple adduct of $\mathbf{L_3H}$ with $GaMe_3$ (probably through the lone pair of the NMe_2 group) and (ii) compound **9** (Scheme 2). Dissolving the oil in thf and refluxing for 4 h resulted in increased conversion to compound **9** of 68%, but a prolonged reflux in toluene (16 h) was required in order for complete conversion to compound **9** to occur. This indicated that ligand $\mathbf{L_3H}$ was not very reactive, with long reaction times at high temperatures needed for complete conversion to occur. Reaction of $\mathbf{L_3H}$ with $InMe_3$ followed similar lines, with prolonged reflux at high temperatures needed for full conversion to complex **10**: further evidence that $\mathbf{L_3H}$ does not react quickly with the reactive MMe_3 (M = Ga, In).

Compound **9** was isolated as a gelatinous brown oil with the ^1H NMR spectrum exhibiting the expected differences from that of $\mathbf{L_3H}$, namely, no NH proton in the 11−12 ppm range and a triplet (rather than a doublet of triplets) for the methylene group next to the amide nitrogen. A singlet at 0.02 ppm corresponding to the Ga−Me groups was characteristic of Ga−Me protons. Similarly, compound **10** was also isolated as a gelatinous brown oil with the chemical shifts in the ^1H and $^{13}C\{^1H\}$ NMR spectra occurring at very similar values.

After discovering that ligand $\mathbf{L_3H}$ did react, albeit slowly, in the expected manner with $GaMe_3$, a freshly prepared solution of $[GaH_3(NMe_3)]$ in Et_2O was added to an ethereal solution of $\mathbf{L_3H}$ (Scheme 2). A small amount of gas was given off, and a color change to pale yellow-green was observed, along with the formation of a white solid. After removing the Et_2O, extracting the solid into hexane afforded a yellow-green oil in 35% yield, which had a broad peak at 5.50 ppm in the ^1H NMR spectrum, characteristic of gallium hydrides. The ^1H NMR spectrum of compound **11** contained the expected peaks for the ligand coordinated to a metal, notably a lack of amine NH and a triplet for the methylene group next to the amide N^-. However, it proved impossible to crystallize compound **11**; thus it was not possible to confirm the solid state structure, although a five-coordinate species with three coordination sites occupied by $\mathbf{L_3}$ and two hydrides is likely observed on the basis of mass spectrometric and NMR spectroscopic data.

In an attempt to improve on the low yield of compound **11**, an alternative synthesis was employed. By forming the hydrochloride salt of ligand $\mathbf{L_3H}$, it was possible to react $\mathbf{L_3H{\cdot}HCl}$ directly with $LiGaH_4$ instead of going through the intermediate $[GaH_3(NMe_3)]$. A white solid in a green solution was again produced, and after removing the Et_2O and extracting the residue into hexane, a viscous green-yellow oil was isolated in an improved 61% yield. Upon standing overnight at RT, colorless crystals formed which were suitable for X-ray diffraction analysis. Unfortunately, the crystals turned out to be the unreacted hydrochloride salt $\mathbf{L_3H{\cdot}HCl}$ (Figure S2, Supporting Information).

In an attempt to form a crystalline gallium hydride complex analogous to compound **11**, it was thought that adding steric bulk to the ligand backbone would result in a solid product. Thus, an ethereal solution of ligand $\mathbf{L_4H}$ was reacted with a freshly prepared solution of $[GaH_3(NMe_3)]$ in Et_2O (Scheme 2). The reaction proceeded as expected, and compound **12** was isolated in 54% yield as a yellow-green oil. Although compound **12** was significantly more viscous than compound **11** (consistent with the higher viscosity of $\mathbf{L_4H}$ compared to $\mathbf{L_3H}$), it was still oily and could not be crystallized. Nonetheless, strong indications that compound **12** had been made were found in the ^1H NMR spectrum where signals characteristic of the coordinated β-ketoiminate were observed, namely, no NH signal at 11.9 ppm and a triplet at 3.22 ppm for the methylene group next to the amide nitrogen.

The Ga/O ratio in complexes **11** and **12** is only 1:1, but for Ga_2O_3 the ratio is 1:1.5. In order to synthesize a precursor, which would not afford oxygen-deficient films, attempts were made to react a second equivalent of $\mathbf{L_3H}$ with complex **11**. However, when one equivalent of $\mathbf{L_3H}$ was added to a toluene solution of **11**, no reaction occurred. Adding excess $\mathbf{L_3H}$ had no effect, and refluxing the reaction merely led to decomposition of **11**, with the formation of metallic gallium. Similar results were obtained with ligand $\mathbf{L_4}$ and complex **12**. Although the formation of oxygen-deficient films is undesirable, postdeposition annealing of films in the air is known to afford stoichiometric Ga_2O_3.[33]

Unfortunately, due to compounds **9**−**12** all being oils, elemental analysis could not be carried out under anaerobic conditions. Attempting elemental analysis rapidly under aerobic conditions only resulted in decomposition. However, the purity of these complexes has been confirmed via ^1H and $^{13}C\{^1H\}$ NMR spectroscopy and also mass spectrometry, where the molecular ion was observed for all compounds.

With gallium β-ketoiminate hydride complexes **11** and **12** in hand, attention turned to the synthesis of indium hydride analogues. Ligand $\mathbf{L_3H}$ was reacted with a freshly prepared ethereal solution of $[InH_3(NMe_3)]$ at −78 °C, but upon warming to RT a gray precipitate of indium metal formed: ^1H NMR spectroscopic analysis of the solution only revealed the presence of $\mathbf{L_3H}$. A similar result was obtained when $\mathbf{L_4H}$ was used. Further investigations into the reaction between $[InH_3(NMe_3)]$ and β-ketoimine ligands revealed that the onset of formation of In metal in each case was *ca.* −30 °C, a

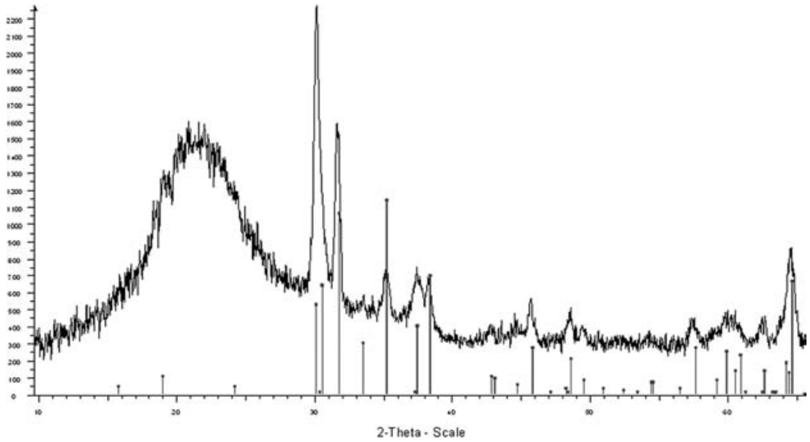

Figure 4. XRD pattern of the film deposited on quartz by AACVD of compound **8** after annealing at 1000 °C for 12 h, consistent with crystalline Ga_2O_3 (solid bars).

similar temperature to the known decomposition temperature of $[InH_3(NMe_3)]$.[34] This could possibly indicate that the β-ketoimine ligands are insufficiently reactive at low temperatures (−78 °C), and the indium hydride starting material decomposes before any reaction with the ligand can take place.

Chemical Vapor Deposition. Anticipating that the use of hydride ligands would enhance the volatility of gallium-containing precursors, compounds **8** and **11** were used as precursors to thin films of Ga_2O_3. Initial studies were carried out using a simple low pressure (LP)CVD tube furnace, but it was found that the compounds decomposed before any significant sublimation occurred and no films were obtained. In order to get the precursors into the reactor, attention turned to using aerosol-assisted (AA)CVD instead. This setup uses a solution of the precursor (usually in toluene) which is nebulized and carried into the reactor chamber using a stream of N_2, whereby the solvent evaporates leaving the precursor to decompose onto the substrate.

The best deposition conditions were found to be 1 L min^{-1} of N_2 carrier gas and a substrate temperature of 450 °C. The films grown using compound **11** as a precursor were patchy and poorly adherent to the substrate, with a large amount of white powdery deposit observed. Powder X-ray diffraction (XRD) showed the films to be amorphous, as is expected from gallium oxide grown at low temperatures. Energy dispersive X-ray (EDX) analysis of the film showed that gallium was present, but the film was too thin to calculate the Ga/O ratio because breakthrough to the underlying glass substrate took place. Altering the deposition conditions did not result in the formation of better-quality films; hence, compound **11** was abandoned as an unsuitable precursor.

Films grown from compound **8** proved to be of much better quality. The coverage of the substrate was much improved with a transparent, adherent film deposited on the bottom plate, and a small amount of white powdery material also deposited onto the top plate, which is the glass plate that rests 8 mm above the surface of the substrate. Deposition on the substrate and top plate is due to the thermophoretic force that gas-phase particles are subjected to during AACVD. Since the flow of gas in the reactor is laminar rather than turbulent, thermophoresis is usually the dominant force in determining the deposition location of particles; hence, deposition also occurs on the elevated surfaces above the actual surface that requires coating. The top plate was measured to be ~50−70 °C lower in temperature than the bottom plate. Films deposited on the substrate were used in the analysis below.

Powder XRD analysis of the as-deposited transparent film revealed that the material was amorphous, but depositing on quartz and annealing in the air at 1000 °C for 12 h resulted in the formation of a crystalline film of Ga_2O_3 (Figure 4). EDX analysis of the as-deposited film again showed breakthrough to the glass substrate making calculation of an accurate Ga/O ratio difficult, although the presence of gallium in the films was confirmed. SEM images showed that the as-deposited film was composed of aggregated spherical globules (Figure 5), but after annealing, the film composition became much smoother and more uniform, with few globular surface features.

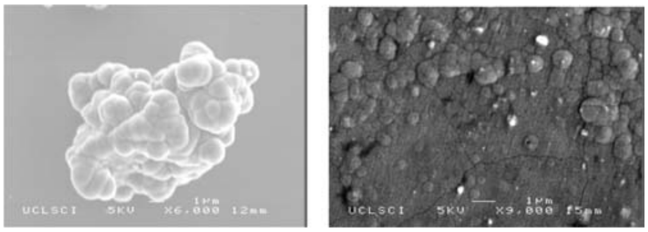

Figure 5. SEM images of the film obtained by AACVD of a toluene solution of **8** on (a) glass and (b) quartz. The quartz film was annealed at 1000 °C for 4 h.

The optical properties of the films deposited from **8** were studied by UV/visible spectroscopy between 90 and 1100 nm. Conducting a Tauc plot of the UV/visible data indicated that the band gap of the films deposited from **8** were ~4.65 eV, which provides further support for the formation of Ga_2O_3 since the band gap of gallium oxide is ~4.2−4.7 eV. Transmission and reflectance measurements between 200 and 2550 nm showed that the films displayed minimal reflectivity (5−10%) and were highly transparent, as shown in Figure 6 with transparency ranges from 80% to 90% in the visible. Previous deposition of Ga_2O_3 *via* AACVD of dialkylalkoxogallanes of the type $[R_2Ga(OR')]_2$ (R = Me, Et; R′ = $CH_2CH_2NMe_2$, CH_2CH_2OMe, etc.) typically resulted in the deposition of gray or brown films indicative of carbon contamination, probably due to the retention of carbon from the Ga−C bond.[32,33,35] In contrast, compound **8** afforded transparent films (as deposited), suggesting minimal carbon contamination. Indeed, no carbon was detected via EDX

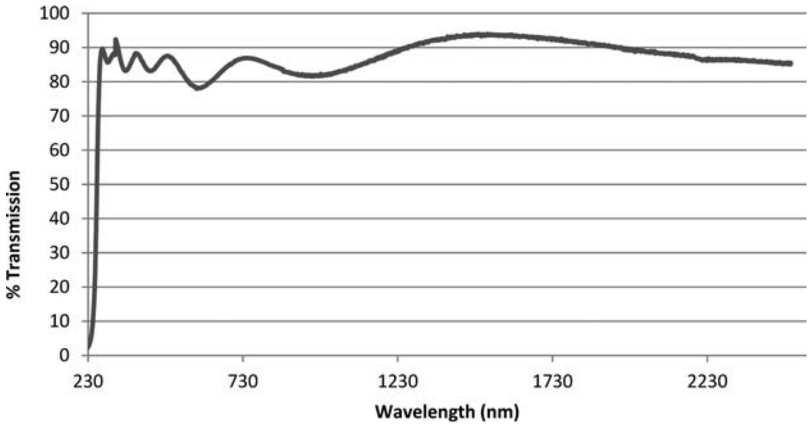

Figure 6. Vis/IR transmission spectra of a film obtained by AACVD of a toluene solution of **8**.

analysis, so carbon contamination levels as a direct result of the precursors used are low (<5 at.%), which could be attributed to the presence of the hydride ligand in **8** resulting in minimal contamination.

CONCLUSIONS

In conclusion, we have demonstrated that it is possible to synthesize a wide range of β-ketoimine ligands and attach them to group 13 metals. The synthesis of gallium β-ketoiminate hydrides can be accomplished by reacting the free ligand directly with $[GaH_3(NMe_3)]$, but analogous indium complexes cannot be made, with indium β-ketoiminate chloride complexes proving to be unreactive toward hydride sources (as well as even more reactive species such as C_8K). Gallium hydride complexes **8** and **11** have been used as precursors to thin films of gallium oxide. Compound **8** proved the superior precursor, affording transparent, adherent films. Extension of the β-ketoiminate chemistry to other main group metals is currently in progress.

EXPERIMENTAL SECTION

All reactions involving metal complexes were carried out under nitrogen using standard Schlenk and glovebox techniques. $AlCl_3$ was obtained from Acros Organics. $GaCl_3$ (10 mesh beads, 99.99%), LiH, and amines were bought from Sigma Aldrich, β-diketones and $InCl_3$ from Alfa Aesar: all were used without further purification. $GaMe_3$ and $InMe_3$ were supplied by SAFC Hitech Ltd. $[GaH_3(NMe_3)]$[21] and $[InH_3(NMe_3)]$,[34] along with ligands $\mathbf{L_1H_2}$ and $\mathbf{L_2H_2}$,[26,27] were synthesized according to literature procedures. Details of the ligand syntheses, sodium salt formation, and compounds **5a** and **5·thf** are contained in the Supporting Information.

^{1}H and ^{13}C{^{1}H} NMR spectra were obtained on a Bruker AMX-400 spectrometer, operating at 295 K and 400.12 MHz (^{1}H). Signals are reported relative to $SiMe_4$ (δ = 0.00 ppm), and the following abbreviations are used: s (singlet), d (doublet), t (triplet), m (multiplet), br (broad). Deuterated solvents were obtained from Goss Scientific and were dried and degassed over molecular sieves prior to use. Mass spectra were obtained using a Micromass 70-SE spectrometer using chemical ionization (CI) with methane reagent gas. The expected pattern for each $[M]^+$ reported was observed. Elemental analyses were obtained at UCL.

[Al(L$_1$)Cl] (3). Compound **1** (540 mg, 2.0 mmol) was suspended in hexane (20 mL) and added slowly to a solution of $AlCl_3$ (270 mg, 2.0 mmol) in hexane (20 mL) at −78 °C. The reaction was stirred for 30 min, then warmed to RT and stirred for 16 h. After this time, solvents were removed, the solid extracted into toluene and filtered. The resulting yellow solution was cooled to −18 °C, affording 200 mg of a yellow crystalline material (35% yield).

δ_H (400.1 MHz, $CDCl_3$): 5.04 (2H, s, CH), 3.21 and 2.65 (each 2H, br s, CH_2), 1.99 (6H, s, $COCH_3$), 1.43 (6H, s, $CNCH_3$) ppm.

δ_C (100.6 MHz, $CDCl_3$): 180.6 (CO), 173.6 (CN), 100.7 (CH), 45.8 (CH_2), 25.8 (CH_3, $COCH_3$), 22.4 (CH_3, $CNCH_3$) ppm.

Mass spec (*m*/*z*): 284 $[M]^+$, 249 $[M - Cl]^+$.

Analysis Calcd. for $C_{12}H_{18}N_2O_2AlCl$: C, 50.62; H, 6.37; N, 9.84. Found: C, 50.71; H, 6.49; N, 9.28.

[Ga(L$_1$)Cl] (4). A suspension of compound **1** (2.68 g, 10.0 mmol) in thf (40 mL) was added to a solution of $GaCl_3$ (1.76 g, 10.0 mmol) in thf (20 mL) at −78 °C and stirred for 30 min. The reaction was warmed to RT then refluxed for 16 h. After this time, the reaction was cooled and filtered and the resulting NaCl extracted with thf. The filtrates were combined, and solvents were removed *in vacuo*. The resulting yellow solid was dissolved in minimal CH_2Cl_2 (*ca.* 10 mL) and precipitated out by the rapid addition of hexane, affording 2.29 g of complex **4** in 70% yield.

δ_H (400.1 MHz, $CDCl_3$): 5.26 (2H, s, CH), 3.62 and 3.51 (each 2H, m, CH_2), 2.08 (6H, s, $COCH_3$), 2.02 (6H, s, $CNCH_3$) ppm.

δ_C (100.6 MHz, $CDCl_3$): 183.6 (CO), 173.3 (CN), 98.8 (CH), 45.1 (CH_2), 26.7 (CH_3, $COCH_3$), 22.6 (CH_3, $CNCH_3$) ppm.

Mass spec (*m*/*z*): 326 $[M]^+$, 291 $[M - Cl]^+$.

Analysis Calcd. for $C_{12}H_{18}N_2O_2GaCl$: C, 44.01; H, 5.54; N, 8.55. Found: C, 44.00; H, 5.49; N, 8.26.

[In(L$_1$)Cl] (5). A suspension of compound **1** (2.68 g, 10.0 mmol) in hexane (40 mL) was added to a suspension of $InCl_3$ (2.21 g, 10.0 mmol) in hexane (20 mL) at −78 °C and stirred for 30 min. The reaction was warmed to RT, then refluxed for 16 h. After this time, the reaction was cooled and filtered and the resulting NaCl extracted with hexane. The filtrates were combined, and solvents were removed *in vacuo*. The resulting yellow solid was dissolved in minimal CH_2Cl_2 (*ca.* 10 mL) and crystallized through vapor diffusion of hexane into the CH_2Cl_2 solution, affording 1.67 g of complex **5** in 45% yield

δ_H (400.1 MHz, $CDCl_3$): 5.26 (2H, s, CH), 3.62 and 3.51 (each 2H, m, CH_2), 2.08 (6H, s, $COCH_3$), 2.02 (6H, s, $CNCH_3$) ppm.

δ_C (100.6 MHz, $CDCl_3$): 183.6 (CO), 173.3 (CN), 98.8 (CH), 45.1 (CH_2), 26.7 (CH_3, $COCH_3$), 22.6 (CH_3, $CNCH_3$) ppm.

Mass spec (*m*/*z*): 372 $[M]^+$, 337 $[M - Cl]^+$.

Analysis Calc. for $C_{12}H_{18}N_2O_2InCl$: C, 38.69; H, 4.87; N, 7.52. Found: C, 38.82; H, 5.01; N, 7.46.

[Ga(L$_2$)Cl] (6). A suspension of compound **2** (570 mg, 2.0 mmol) in hexane (30 mL) was cooled to −78 °C and added to a solution of $GaCl_3$ (352 mg, 2.0 mmol) in hexane (20 mL) at −78 °C. The reaction was stirred for 15 min, warmed to RT, and then stirred for 16 h. After this time, the reaction was filtered, solvents removed, and the resulting yellow/brown solid dissolved in minimal CH_2Cl_2 (*ca.* 5 mL) and layered with hexane. Yellow crystals (270 mg) of the title compound formed in 38% yield.

δ_H (400.1 MHz, $CDCl_3$): 5.06 (2H, s, CH), 3.71 and 3.46 (each 2H, br s, NCH_2), 2.01 (6H, s, $COCH_3$), 2.00 (6H, s, $CNCH_3$), 1.87 (2H, quintet, *J* = 6.5 Hz, CH_2) ppm.

Table 2. Crystallographic Data for Structurally Characterized Compounds Reported in This Paper

compound	5	5a	5·thf	6	7	$L_3H\cdot HCl$
chemical formula	$C_{24}H_{36}Cl_2In_2N_4O_4$	$C_{36}H_{56}Cl_2In_2N_6O_6$	$C_{16}H_{26}ClInN_2O_3$	$C_{13}H_{20}ClGaN_2O_2$	$C_{13}H_{20}ClInN_2O_2$	$C_{10}H_{21}ClN_2O$
fw (g mol^{-1})	745.11	969.41	444.66	341.48	386.58	220.74
crystal system	monoclinic	triclinic	monoclinic	triclinic	triclinic	monoclinic
space group	$P2_1/c$	$P\bar{1}$	$P2_1/c$	$P\bar{1}$	$P\bar{1}$	$P2_1$
a (Å)	11.276(4)	8.2191(1)	8.0171(3)	7.4177(9)	8.8098(8)	5.4450(1)
b (Å)	11.797(4)	9.4727(2)	14.7596(5)	8.6862(11)	12.6328(11)	11.4384(3)
c (Å)	12.513(3)	14.0874(2)	17.1126(5)	12.4715(15)	14.7568(13)	10.0709(3)
α (deg)		73.982(1)		72.534(2)	94.327(1)	
β (deg)	120.50(2)	75.889(1)	114.806(2)	75.996(2)	95.448(1)	104.629(2)
γ (deg)		86.436(1)		77.103(2)	110.058(1)	
V (Å^3)	1434.2(8)	1022.39(3)	1838.09(11)	733.82(16)	1525.5(2)	606.90(3)
Z	2	1	4	2	4	2
ρ_{calcd} (g cm^{-3})	1.725	1.574	1.607	1.545	1.683	1.208
μ (mm^{-1})	1.830	1.308	1.446	2.056	1.724	0.289
reflns collected	7466	23101	18466	5937	10370	7150
unique reflns	3268	4701	4201	3152	5135	1447
R_{int}	0.023	0.0395	0.0373	0.0188	0.0166	0.0468
R_1 and wR_2 [I > 2σ(I)]	0.0239, 0.0472	0.0225, 0.0516	0.0320, 0.0601	0.0219, 0.0566	0.0235, 0.0624	0.0874, 0.2442
R_1 and wR_2 [all data]	0.0294, 0.0489	0.0254, 0.0530	0.0421, 0.0651	0.0235, 0.0576	0.0275, 0.0644	0.0888, 0.2449

δ_C (100.6 MHz, $CDCl_3$): 98.8 (CH), 47.2 (NCH_2), 30.3 (CH_2), 26.5 (CH_3, $COCH_3$), 18.8 (CH_3, $CNCH_3$), ppm. (CO) and (CN) not detected.

Analysis Calcd. for $C_{13}H_{20}N_2O_2GaCl$: C, 45.75; H, 5.90; N, 8.20. Found: C, 45.44; H, 6.04; N, 8.28.

[In(L_2)Cl] (7). The procedure described for compound **6** was followed, with $InCl_3$ (442 mg, 2.0 mmol) used in place of $GaCl_3$. Yellow crystals (270 mg) of **7** were isolated in 35% yield.

δ_H (400.1 MHz, $CDCl_3$): 4.94 (2H, s, CH), 3.76 and 3.47 (each 2H, br s, NCH_2), 2.63 (2H, br s, CH_2), 2.02 (6H, s, $COCH_3$), 1.99 (6H, s, $CNCH_3$) ppm.

δ_C (100.6 MHz, $CDCl_3$): 185.8 (CO), 176.0 (CN), 98.0 (CH), 51.9 (NCH_2), 29.1 (CH_2), 27.6 (CH_3, $COCH_3$), 23.2 (CH_3, $CNCH_3$) ppm.

Mass spec (m/z): 386 $[M]^+$, 351 $[M - Cl]^+$, 238 $[\mathbf{L_2H_2}]^+$.

Analysis Calcd. for $C_{13}H_{20}N_2O_2InCl$: C, 40.39; H, 5.21; N, 7.25. Found: C, 40.17; H, 5.30; N, 7.59.

[Ga(L_1)H] (8). A freshly prepared solution of $[GaH_3(NMe_3)]$ (5.0 mmol) in Et_2O (50 mL) was cooled to −78 °C and added to a suspension of $\mathbf{L_1H_2}$ (1.12 g, 5.0 mmol) in Et_2O (20 mL) at −78 °C. The suspension was stirred for 15 min, then warmed to RT and stirred for 16 h. After this time, a yellow solution with a white suspension had formed. The reaction was filtered, and volatiles were removed *in vacuo*, affording 1.04 g of a yellow solid in 71% yield.

δ_H (400.1 MHz, C_6D_6): 5.56 (1H, v br s, GaH), 4.80 (2H, s, CH), 2.80−2.89 and 2.58−2.68 (each 2H, m, CH_2), 1.90 (6H, s, $COCH_3$), 1.39 (6H, s, $CNCH_3$) ppm.

δ_C (100.6 MHz, C_6D_6): 182.45 (CO), 171.25 (CN), 97.62 (CH), 45.28 (CH_2), 26.70 (CH_3, $COCH_3$), 21.52 (CH_3, $CNCH_3$) ppm.

Analysis Calcd. for $C_{12}H_{19}N_2O_2Ga$: C, 35.69; H, 6.99; N, 6.94. Found: C, 35.75; H, 6.91; N, 7.06.

[Ga(L_3)Me_2] (9). A solution of $GaMe_3$ (574 mg, 5.0 mmol) in toluene (30 mL) was cooled to −78 °C, and ligand $\mathbf{L_3H}$ (920 mg, 5.0 mmol) was added dropwise. The solution was gradually warmed to RT with the evolution of methane gas, then refluxed for 16 h. After this time, solvents were removed, affording 1.35 g of a gelatinous brown liquid in 95% yield.

δ_H (400.1 MHz, C_6D_6): 4.67 (1H, s, CH), 3.13 (2H, t, J = 7.5 Hz, NCH_2), 1.94−1.99 (8H, m, Me_2NCH_2 + $N(CH_3)_2$), 1.85 (3H, s, $COCH_3$), 1.51 (3H, s, $CNCH_3$), 1.49 (2H, quintet, J = 7.0 Hz, CH_2), 0.02 (6H, s, $GaCH_3$) ppm.

δ_C (100.6 MHz, C_6D_6): 180.43 (CO), 171.46 (CN), 97.96 (CH), 56.67 (NCH_2), 46.80 (Me_2NCH_2), 45.30 ($N(CH_3)_2$), 28.32 (CH_2), 26.35 (CH_3, $COCH_3$), 20.53 (CH_3, $CNCH_3$), −6.78 (CH_3, $GaCH_3$) ppm.

Mass spec (m/z): 283 $[M]^+$.

[In(L_3)Me_2] (10). The procedure for compound **9** was followed with $InMe_3$ (800 mg, 5.0 mmol) being used in place of $GaMe_3$. A total of 1.51 g of complex **10** was isolated as a gelatinous brown liquid in 92% yield.

δ_H (400.1 MHz, C_6D_6): 4.81 (1H, s, CH), 3.04 (2H, t, J = 6.0 Hz, NCH_2), 2.00 (3H, s, $COCH_3$), 1.93 (2H, t, J = 6.0 Hz, Me_2NCH_2), 1.76 [6H, s, $N(CH_3)_2$], 1.56 (3H, s, $CNCH_3$), 1.25 (2H, quintet, J = 6.0 Hz, CH_2), 0.00 (6H, s, $InCH_3$) ppm.

δ_C (100.6 MHz, C_6D_6): 183.90 (CO), 171.67 (CN), 97.59 (CH), 58.38 (NCH_2), 49.15 (Me_2NCH_2), 45.38 [$N(CH_3)_2$], 28.06 (CH_3, $COCH_3$), 27.89 (CH_2), 21.03 (CH_3, $CNCH_3$), −6.78 (CH_3, $InCH_3$) ppm.

Mass spec (m/z): 328 $[M]^+$.

[Ga(L_3)H_2] (11). (Method 1) A freshly prepared solution of $[GaH_3(NMe_3)]$ (5.0 mmol) in Et_2O (30 mL) was cooled to −78 °C, and ketoimine $\mathbf{L_3H}$ (920 mg, 5.0 mmol) was added dropwise. A white precipitate formed; the suspension was warmed to RT and stirred for 16 h. After this time, solvents were removed, the solid extracted with hexane (2 × 20 mL), and the hexane extracts concentrated, affording 446 mg of a yellow-green oil in 35% yield.

(Method 2) A freshly prepared solution of $LiGaH_4$ (5.0 mmol) in Et_2O (30 mL) at −78 °C was added to $\mathbf{L_3H\cdot HCl}$ (1.10 g, 5.0 mmol). The reaction was stirred for 15 min, warmed to RT, and stirred for 16 h. After this time, solvents were removed and the solid extracted with hexane (3 × 20 mL), and the hexane extracts were combined and concentrated, affording 777 mg of a yellow oil in 61% yield.

δ_H (400.1 MHz, C_6D_6): 5.50 (2H, v br s, GaH), 4.69 (1H, s, CH), 3.08 (2H, t, J = 7.0 Hz, NCH_2), 1.97 (2H, m, Me_2NCH_2), 1.94 [6H, s, $N(CH_3)_2$], 1.82 (3H, s, $COCH_3$), 1.46−1.49 (2H, m, CH_2), 1.45 (3H, s, $CNCH_3$) ppm.

δ_C (100.6 MHz, C_6D_6): 181.14 (CO), 172.30 (CN), 98.40 (CH), 56.48 (NCH_2), 47.71 (Me_2NCH_2), 45.19 [$N(CH_3)_2$], 27.23 (CH_2), 26.20 (CH_3, $COCH_3$), 20.61 (CH_3, $CNCH_3$) ppm.

Mass spec (m/z): 255 $[M]^+$.

[Ga(L_4)H_2] (12). Procedure 1 for compound **11** was followed, using ketoimine $\mathbf{L_4H}$ (1.54 g, 5.0 mmol). A total of 1.03 g of complex **12** was isolated as a yellow-green oil in 54% yield.

δ_H (400.1 MHz, C_6D_6): 7.87−7.91 (2H, m, Ar), 7.04−7.11 (6H, m, Ar), 6.97−7.01 (2H, m, Ar), 5.81 (1H, s, CH), 5.55 (2H, v br s, GaH), 3.22 (2H, t, J = 7.0 Hz, NCH_2), 2.00 (2H, t, J = 6.0 Hz, Me_2NCH_2), 1.92 [6H, s, $N(CH_3)_2$], 1.42 (2H, quintet, J = 6.5 Hz, CH_2) ppm.

δ_C (100.6 MHz, C_6D_6): 177.31 (CO), 175.10 (CN), 139.53, 139.40 (C, Ar), 130.46, 128.98, 128.59, 128.34, 127.50, 127.27 (CH, Ar), 96.95 (CH), 57.51 (NCH$_2$), 51.32 (CH$_2$, Me$_2$NCH$_2$), 45.14 [N(CH$_3$)$_2$], 28.49 (CH$_2$) ppm.

Mass spec (m/z): 379 [M]$^+$.

AACVD. For AACVD experiments, nitrogen (99.99%) was obtained from BOC and used as supplied. Depositions were obtained on SiCO barrier layer (50 nm) float-glass of dimensions *ca.* 90 mm × 45 mm × 4 mm. Prior to use, the glass substrates were cleaned using petroleum ether (60−80 °C) and ^{i}PrOH, then dried in the air. The precursor (*ca.* 300 mg) was dissolved in toluene (*ca.* 30 mL) and vaporized at room temperature by use of a PIFCO ultrasonic humidifier. The aerosol was carried into the reactor using nitrogen through a brass baffle to obtain a laminar flow. A graphite block containing a Whatman cartridge heater was used to heat the glass substrate. The temperature of the substrate was monitored by a Pt−Rh thermocouple, and the horizontal bed reactor was heated to the required temperature before diverting the nitrogen line through the aerosol and hence to the reactor. The total time for the deposition process was *ca.* 2 h. The coated glass substrate was cut into *ca.* 1 cm × 1 cm squares for subsequent analysis by scanning electron microscopy (SEM).

Film Analysis Methods. X-ray powder diffraction patterns were measured on a Siemens D5000 diffractometer using monochromated Cu Kα radiation (λ = 1.5400 Å). The diffractometer used glancing incident radiation (1.5°). The films on the glass substrates were indexed using Unit Cell and compared to database standards. SEM was carried out on a JEOL 6301 filament scanning electron microscope.

Crystallography. A summary of the crystal data, data collection, and refinement for crystallographically characterized compounds are given in Table 2. The data set for compound **5** was collected at 100(2) K on a *Rigaku AFC12* goniometer equipped with an enhanced sensitivity (HG) *Saturn724+* detector mounted at the window of an *FR-E+ SuperBright* Mo rotating anode generator with VHF *Varimax* optics (70 μm focus). The program used for control and integration was CrystalClear.[37] Data sets for compounds **5a**, **5·thf**, and **L$_3$H·HCl** were collected at 120(2) K on an Enraf-Nonius Kappa CCD area detector diffractometer with an FR591 rotating anode (Mo Kα radiation) in ω scanning mode with ψ and ω scans to fill the Ewald sphere. The programs used for control and integration were Collect, Scalepack, and Denzo.[38,39] Data sets for compounds **6** and **7** were obtained on a Bruker SMART APEX CCD diffractometer using graphite-monochromated Mo Kα radiation at 150(2) K. Data reduction and integration were carried out with SAINT+ and absorption corrections applied using SADABS.[40]

The crystals were mounted on mitogen loops (**5**, **5a**, **5·thf**, **L$_3$H·HCl**) or on a glass fiber with silicon grease (**6**, **7**) from Fomblin. All solutions and refinements were performed using the WinGX package and all software packages within.[41] All non-hydrogen atoms were refined using anisotropic thermal parameters, and hydrogens were added using a riding model. Hydrogens bonded to nitrogen in **5a** and **L$_3$H·HCl** were located in the Fourier difference map and refined isotropically. The compound **L$_3$H·HCl** crystallized in the space group $P2_1$ as a racemic twin. The crystals were small and weakly diffracting, resulting in low C−C bond precision.

■ ASSOCIATED CONTENT

Ⓢ Supporting Information

Experimental and spectroscopic details for the synthesis of ligands **L$_1$H$_2$**, **L$_2$H$_2$**, **L$_3$H**, and **L$_4$H** (and **L$_3$H·HCl**) and spectroscopic data for compounds **5a** and **5·thf** are included as supporting data, along with X-ray crystallographic data in CIF format for the structures of compounds **5**, **5a**, **5·thf**, **6**, **7**, and **L$_3$H·HCl**. This material is available free of charge via the Internet at http://pubs.acs.org.

■ AUTHOR INFORMATION

Corresponding Author

*E-mail: c.j.carmalt@ucl.ac.uk.

Notes

The authors declare no competing financial interest.

■ ACKNOWLEDGMENTS

We would like to thank the EPSRC (grant nos. EP/H00064X/1 and EP/F035675/1), UCL (Impact Studentship Scheme), and the Horshall fund for financial support. We would also like to thank SAFC Hitech Ltd. for supplying GaMe$_3$ and InMe$_3$; Pilkington for supplying the float glass; and Drs. Peter Horton, Mateusz Pitak, and Graham Tizzard at the EPSRC National Crystallography Service for data set collection of **5**, **5a**, **5·thf**, and **L$_3$·HCl**.

■ REFERENCES

(1) Fleischer, M.; Meixner, H. *Sens. Actuators, B* **1993**, *13*, 259.

(2) Liu, Z.; Yamazaki, T.; Shen, Y.; Kikuta, T.; Nakatani, N.; Li, Y. *Sens. Actuators, B* **2008**, *129*, 666.

(3) Fleischer, M.; Meixner, H. *Sens. Actuators, B* **1991**, *5*, 115.

(4) Fleischer, M.; Meixner, H. *Sens. Actuators, B* **1991**, *4*, 437.

(5) Hao, J.; Cocivera, M. *J. Phys. D: Appl. Phys.* **2002**, *35*, 433.

(6) Knapp, C. E.; Pugh, D.; McMillan, P. F.; Parkin, I. P.; Carmalt, C. J. *Inorg. Chem.* **2011**, *50*, 9491.

(7) Carmalt, C. J.; King, S. J. *Coord. Chem. Rev.* **2006**, *250*, 682.

(8) Chi, Y.; Chou, T.-Y.; Wang, Y.-J.; Huang, S.-F.; Carty, A. J.; Scoles, L.; Udachin, K. A.; Peng, S.-M.; Lee, G.-H. *Organometallics* **2004**, *23*, 95.

(9) Basharat, S.; Betchley, W.; Carmalt, C. J.; Barnett, S.; Tocher, D. A.; Davies, H. O. *Organometallics* **2007**, *26*, 403.

(10) Pugh, D.; Bloor, L. G.; Parkin, I. P.; Carmalt, C. J. *Chem.—Eur. J.* **2012**, *18*, 6079.

(11) Mîinea, L.; Suh, S.; Bott, S. G.; Liu, J.-R.; Chu, W.-K.; Hoffman, D. M. *J. Mater. Chem.* **1999**, *9*, 929.

(12) Valet, M.; Hoffman, D. M. *Chem. Mater.* **2001**, *13*, 2135.

(13) Basharat, S.; Knapp, C. E.; Carmalt, C. J.; Barnett, S. A.; Tocher, D. A. *New J. Chem.* **2008**, *32*, 1513.

(14) Bloor, L.; Carmalt, C. J.; Pugh, D. *Coord. Chem. Rev.* **2011**, *255*, 1293.

(15) Oritz, A.; Alonso, J. C.; Andrade, E.; Urbiola, C. J. *J. Electrochem. Soc.* **2001**, *148*, F26.

(16) Peng, Q.; Hojo, D.; Park, K. J.; Parsons, G. N. *Thin Solid Films* **2008**, *516*, 4997.

(17) Wu, P.; Gao, Y.-M.; Kershaw, R.; Dwight, K.; Wold, A. *Mater. Res. Bull.* **1990**, *25*, 357.

(18) Pugh, D.; Bloor, L. G.; Sathasivam, S.; Parkin, I. P.; Carmalt, C. J. *Eur. J. Inorg. Chem.* **2011**, 1953.

(19) Atwood, J. L.; Bott, S. G.; Elms, F. M.; Jones, C.; Raston, C. L. *Inorg. Chem.* **1991**, *30*, 3792.

(20) Jones, C. *Chem. Commun.* **2001**, 2293.

(21) Andrews, P. C.; Gardiner, M. G.; Raston, C. L.; Tolhurst, V.-A. *Inorg. Chim. Acta* **1997**, *259*, 249.

(22) Shen, Y.; Han, J.; Gu, H.; Zhu, Y.; Pan, Y. *J. Organomet. Chem.* **2004**, *689*, 3461.

(23) Lugo, A. F.; Richards, A. F. *Eur. J. Inorg. Chem.* **2010**, *13*, 2025.

(24) Ziemkowska, W.; Kubiak, A.; Kucharski, S.; Wozniak, R.; Anulewicz-Ostrowska, R. *Polyhedron* **2007**, *26*, 1436.

(25) Vohs, J. K.; Miller, D. O.; Denomme, D. R.; Ziller, J. W.; Fahlman, B. D. *Acta Crystallogr.* **2005**, *C61*, m287.

(26) Bresciani-Pahor, N.; Calligaris, M.; Nardin, G.; Randaccio, L.; Viterbo, D. *Acta Crystallogr.* **1979**, *B35*, 2776.

(27) Elerman, Y.; Kabak, M.; Kara, H.; Güven, K.; Nakipoğlu, C. *Acta Crystallogr.* **1999**, *C55*, 1508.

(28) Addison, A. W.; Rao, T. N.; Reedijk, J.; van Rijn, J.; Verschoor, G. C. *J. Chem. Soc., Dalton Trans.* **1984**, 1349.

(29) Baker, R. J.; Jones, C.; Junk, P. C.; Kloth, M. *Angew. Chem., Int. Ed.* **2004**, *43*, 3852.

(30) Abernethy, C. D.; Cole, M. L.; Jones, C. *Organometallics* **2000**, *19*, 4852.

(31) Basharat, S.; Carmalt, C. J.; King, S. J.; Peters, E. S.; Tocher, D. A. *Dalton Trans.* **2004**, 3475.

(32) Knapp, C. E.; Pemberton, L.; Carmalt, C. J.; Pugh, D.; McMillan, P. F.; Barnett, S. A.; Tocher, D. A. *Main Group Chem.* **2010**, *9*, 31.

(33) (a) Basharat, S.; Carmalt, C. J.; Palgrave, R.; Barnett, S. A.; Tocher, D. A.; Davies, H. O. *J. Organomet. Chem.* **2008**, *693*, 1787. (b) Basharat, S.; Carmalt, C. J.; Binions, R.; Palgrave, R.; Parkin, I. P. *Dalton Trans* **2008**, 591.

(34) Hibbs, D. E.; Hursthouse, M. B.; Jones, C.; Smithies, N. A. *Chem. Commun.* **1998**, 869.

(35) (a) Knapp, C. E.; Hyett, G.; Parkin, I. P.; Carmalt, C. J. *Chem. Mater.* **2011**, *23*, 1719. (b) Knapp, C. E.; Kafizas, A.; Parkin, I. P.; Carmalt, C. J. *J. Mater. Chem.* **2011**, *21*, 12644.

(36) Coles, S. J.; Gale, P. A. *Chem. Sci* **2012**, *3*, 683.

(37) *CrystalClear-SM-Expert_2.0*; Rigaku Corporation: Tokyo, 2011.

(38) Hooft, R.; *COLLECT Nonius BV*; Nonius BV: Delft, The Netherlands: 1997−2000.

(39) Otwinowski, Z.; Minor, W.; Scalepack, D. *Methods Enzymol.* **1997**, 276.

(40) *SMART*; *SAINT*; *SADABS*; Bruker AXS Inc.: Madison, WI, 1998.

(41) Farrugia, L. J. *J. Appl. Crystallogr.* **1999**, *32*, 83.